DOI: 10.1002/chem.200501119

Kinetic Energy Release of C_{70}^+ and Its Endohedral Cation $N@C_{70}^+$: Activation Energy for N Extrusion

Baopeng Cao,*[a, b] Tikva Peres,[b] Chava Lifshitz,[b] R. James Cross,*[c] and Martin Saunders[c]

Abstract: Unimolecular decomposition of C_{70}^+ and its endohedral cation $N@C_{70}^+$ were studied by high-resolution mass-analyzed ion kinetic energy (MIKE) spectrometry. Information on the energetics and dynamics of these reactions was extracted. C_{70}^+ dissociates unimolecularly by loss of a C_2 unit, whereas $N@C_{70}^+$ expels the endohedral N atom. Kinetic energy release distributions (KERDs) in these reactions were measured. By use of finite heat bath theory (FHBT), the binding energy for C_2 emission from C_{70}^+ and the activation energy for N elimination from $N@C_{70}^+$ were deduced from KERDs in the light of a recent finding that fragmentation of fullerene cations proceeds via a very loose transition state. The activation energy measured for N extrusion from $N@C_{70}^+$ was found to be lower than that for C_2 evaporation, higher than the value from its neutral molecule $N@C_{70}$ obtained on the basis of thermal stability measurements, and coincident with the theoretical value. The results provide confirmation that the proposed extrusion mechanism in which the N atom escapes from the cage via formation of an aza-bridged intermediate is correct.

Keywords: cations · cluster compounds · fullerenes · kinetics · reaction mechanisms

Introduction

Endohedral fullerenes have attracted special attention because of their unique structures and novel properties that are absent for empty fullerenes. Evidence that nonmetallic atoms can be encaged inside the hollow space of C_{60} and C_{70} was first obtained by Schwarz et al. in high-energy collision experiments,[1] and later confirmed by macroscopic synthesis of endohedral fullerenes with noble gas atoms trapped inside.[2] The techniques for incorporation of nonmetallic atoms into fullerenes involve application of high temperature and high pressure[2] and ion implantation.[3] C_{60}, C_{70}, and their derivatives are employed as starting materials to accommodate the guest atoms. The typical doping yield achieved by these methods is around a small fraction of 1%. To elucidate the encapsulation of nonmetallic atoms inside fullerenes, a mechanism for incorporation and release of the guest atom was proposed that involves reversible breaking of a bond to open a window in the cage.[4] Recently, 100% doping yield was finally achieved through a window opened by chemical "surgery" on C_{60} cage.[5] Neutral molecules or atoms such as He, Ne, Ar, Kr, Xe, N, P, N_2, H_2, CO, H_2O, and HeNe have thus far been encapsulated inside C_{60} or C_{70}.[2–7]

Among the fascinating endohedral compounds are $N@C_{60}$ and $N@C_{70}$, which have an intrinsically very reactive N atom.[7–9] In these compounds the inert interior surface of the fullerene furnishes an ideal chemical Faraday trap that leaves the encapsulated N atom in its high-spin ground state.[7–10] The N atom is located at or very close to the center of the cage and is stabilized by the fullerene cage. Electron paramagnetic resonance and theoretical studies on these endohedral fullerenes disclosed that electron transfer between the endohedral N atom and its chemical surroundings hardly occurs and no covalent bond exists.[7–10] The full-

[a] Dr. B. Cao
Department of Chemistry, Indiana University
800 East Kirkwood Avenue, Bloomington, IN 47404 (USA)
Current address:
Center for Tsukuba Advanced Research Alliance
University of Tsukuba, Tsukuba 305-8577 (Japan)
Fax: (+81) 29-853-7289
E-mail: bcao@tara.tsukuba.ac.jp

[b] Dr. B. Cao, T. Peres, Prof. Dr. C. Lifshitz
Department of Physical Chemistry and The Farkas Center for Light Induced Process
The Hebrew University of Jerusalem, Jerusalem 91904 (Israel)

[c] Prof. Dr. R. J. Cross, Prof. Dr. M. Saunders
Department of Chemistry, Yale University
New Haven, CT 06521-8170 (USA)
Fax: (+1) 203-432-6144
E-mail: james.cross@yale.edu

erene cages provide a "zero-interaction" inert environment that defines the rotational and vibrational states of the endohedral atom well and results in a "cold" N atom ready for spectroscopic investigation.[11] The relative isolation of the spin of the N atom affords an opportunity for investigating the atomic state of nitrogen in a quantum snare and makes these fullerene-based molecules possible candidates for use as qubits in electron-spin-based quantum computers.[12]

These remarkable molecules are usually produced by ion bombardment of C_{60} and C_{70}.[7–9] The molar ratio of incorporation ($N@C_{60}/C_{60}$) achieved by ion implantation is normally around 10^{-4}–10^{-6}, which is too low to be directly subjected to other spectroscopic investigations, except for the EPR and ENDOR techniques, which are very sensitive in mapping the spin and even the charge distribution. These remained the only two experimental spectroscopic methods for characterizing these compounds until a sample enriched in $N@C_{60}$ was obtained by use of an HPLC separation system in 2002.[13a] A breakthrough in complete isolation of pure $N@C_{60}$ and $N@C_{70}$ was finally achieved by Jakes et al.[13b] and later by Kamai et al.,[14] paving the way to completely study these unique molecules with spectroscopic techniques other than EPR and ENDOR.

Investigations on $N@C_{60}$ and $N@C_{70}$ have thus far focused on the atomic state of the incarcerated N atom and the effect of fullerene cage on it.[7–13] Less attention has been paid to the influence on the cage of incorporation of the nitrogen atom.[6,14–15] It is of interest whether the two most abundant fullerenes, C_{60} and C_{70}, are modified by introduction of the extremely reactive N atom. Investigations on pure $N@C_{60}$ by Dinse et al. demonstrated that $N@C_{60}$ has a UV/Vis absorption spectrum indistinguishable from that of C_{60} within experimental uncertainty,[13b] that is, the coupling between the molecular wavefunctions of N and C_{60} is negligible. Recent studies have unveiled that incorporation of the N atom lowers the photochemical reactivity of C_{60} toward disilirane.[15] We have studied the unimolecular dissociation of $N@C_{60}^+$ and $N_2@C_{60}^+$ using mass-analyzed ion kinetic energy (MIKE) spectrometry[6,16] and found the N atom does not destabilize C_{60}. In sharp contrast to $N_2@C_{60}$ and other endohedral fullerenes that dissociate by loss of a C_2 unit via the Rice cage shrink–wrap mechanism, $N@C_{60}^+$ instead expels the endohedral N atom. The activation energy for N evaporation from $N@C_{60}^+$ was extracted on a very loose basis, and the value is too high with respect to the theoretical one and needs further evaluation on a firmer basis. Here we report new experimental approaches to the energetics and dynamics of the unimolecular decomposition of C_{70}^+ and $N@C_{70}^+$. Mass-analyzed ion kinetic energy spectra and kinetic energy releases of the reaction were measured, and dissociation channels of these cations are disclosed. The activation energy for N extrusion from $N@C_{70}^+$ and the binding energy for C_2 loss from C_{70}^+, determined here in the light of a recent finding that fragmentation of fullerene cations proceeds via a very loose transition state, agree with theoretical values. The results unveil the reason why $N@C_{70}^+$ extrudes the endohedral N atom rather than a C_2 unit and confirm that the mechanism for N extrusion via an aza-bridged intermediate is correct.

Results and Discussion

Mass spectrum of $N@C_{70}$: Figure 1 shows the mass spectrum of a mixture produced by bombarding C_{70} with N^+ ions. In addition to the peaks at *m/z* 840–845 that correspond to undoped C_{70}, a series of small peaks beginning at *m/z* 854 was observed. These peaks are the unique signature of $N@C_{70}$. The ratio of filled to empty C_{70} is about 0.33%, which is much higher than the doping yield of $N@C_{60}$.[6] The EPR spectrum of $N@C_{70}$ shows three narrow lines, in accordance with the endohedral nature of the N atom. The concentration of $N@C_{70}$ obtained on the basis of EPR analysis is nearly the same as the value from mass spectroscopic analysis.

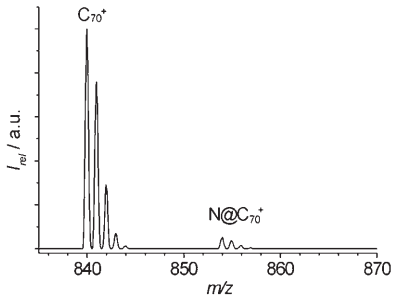

Figure 1. Mass spectrum of a mixture of $N@C_{70}$ and C_{70}: electron ionizing energy 70 eV, emission current 5 mA, ion source temperature 200 °C.

Under optimized conditions the incorporation yield for $N@C_{70}$ is much higher than that for $N@C_{60}$. This is probably due to the difference in C_2 binding energy between C_{60} and C_{70}. According to the window mechanism proposed for incorporation and release of a nonmetallic atom,[4] the N^+ ion is incorporated into a fullerene cage by first breaking a bond to open a window in the cage, then entering through the opening, and finally closing the window. The C_2 binding energy of a fullerene cage provides information on how readily a bond in the cage can be broken and therefore furnishes a hint about the ease of opening the window. The observation that C_{70} is easier to dope than C_{60} signifies that C_{70} may have a lower C_2 binding energy than C_{60}. This is the case: the measured C_2 evaporation energy of C_{70} is indeed about 0.8 eV lower than that of C_{60} (see below).

The energy inherited from the N^+ ion during collision with fullerene cages may also cause a difference in synthesis yield between $N@C_{60}$ and $N@C_{70}$. When an N^+ ion that has been accelerated before being encaged is shot into C_{60} or C_{70}, about 200 eV of energy is transferred from the N^+ ion to the newly generated endohedral fullerene, and this energy is concentrated in a single molecule. To form a stable product, this huge amount of energy must be rapidly trans-

ferred to neighboring molecules, or else the newly formed $N@C_{60}$ or $N@C_{70}$ will decompose. Since C_{70} is larger, it has more vibrational degrees of freedom and therefore a longer lifetime for decomposition. This means that $N@C_{70}$ is intrinsically more likely to survive than $N@C_{60}$, that is, the relaxation process after formation may cause more decomposition of $N@C_{60}$ and result in a lower yield of $N@C_{60}$ than $N@C_{70}$.

In the mass spectrum of $N@C_{70}$ the isotopic peaks contributed by ^{13}C are thoroughly resolved, so it is easy to select only one mass for MIKE measurement. The MIKE spectra thus measured will be free of isotopic effects, and their shapes will be Gaussian. This is the case for the current studies of C_{70} and $N@C_{70}$ and for the previous investigation on $N@C_{60}$ (see below).

MIKE spectra of C_{70}^+ and $N@C_{70}^+$: MIKE spectra for a unimolecular reaction reveal kinetic energy release distributions (KERDs) in the reaction, and therefore information on the dynamics and energetics of the reaction can be extracted from MIKE spectra.[17] MIKE scans of C_{70}^+ and $N@C_{70}^+$ ions were performed on the mass of the most intense isotope, that is, *m/z* 840 for C_{70} and 854 for $N@C_{70}$. Peak shapes of metastable ions were determined by scanning the electrostatic analyzer and using the single-ion counting that was achieved by combination of an electron multiplier, amplifier/discriminator, and multichannel analyzer.[18] Figures 2

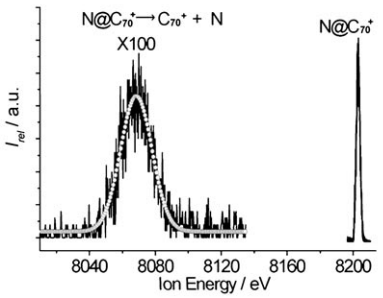

Figure 2. MIKE spectra for unimolecular extrusion of the N atom from $N@C_{70}^+$ (*m/z* 854). The narrow peak (right) is the parent ion. The broad peak (left) is the daughter ion (solid line: experimental data, open circles: Gaussian fit). The energy broadening on the laboratory scale for the metastable ions is due to the kinetic energy release in the center of mass (CM) scale of the parent ion dissociation taking place in the second field-free region (ff2) of the VG-ZAB-2f instrument.

and 3 show the high-resolution MIKE spectra for unimolecular decomposition of $N@C_{70}^+$ and C_{70}^+, the corresponding parent peaks, and Gaussian fits to the MIKE spectra. In Figure 2 the metastable peak for unimolecular dissociation of $N@C_{70}^+$ (C_{70}^+ generated from $N@C_{70}^+$, left, solid line: experimental, open circles: Gaussian fit) is drawn to the same laboratory ion-energy scale as its parent peak ($N@C_{70}^+$, right) to show their relationship in width. Clearly, the daughter-ion peak is very broad, whereas the parent-ion peak is narrow. The energy broadening of metastable ions is due to the kinetic energy release in the center of mass (CM)

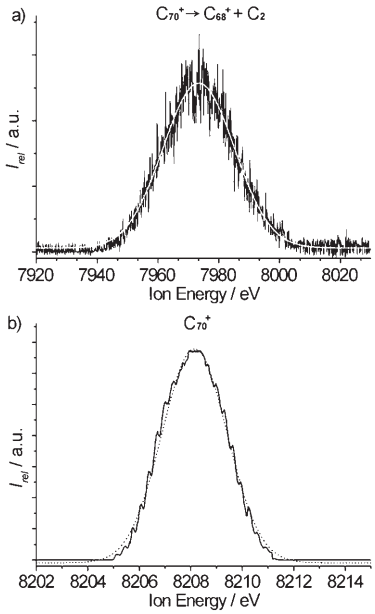

Figure 3. MIKE spectra for unimolecular loss of a C_2 unit from C_{70}^+ (*m/z* 840). a) Peak shape of metastable ion (black line: experimental data, white line: Gaussian fit). b) Parent-ion peak shape (solid line: experimental data, dotted line: Gaussian fit). Both the parent- and daughter-ion peak shapes are Gaussian.

Unimolecular dissociation channels of C_{70}^+ and $N@C_{70}^+$: In principle there should be competition in the unimolecular reaction of endohedral fullerenes between elimination of an endohedral atom and loss of a C_2 unit from the cage. MIKE spectrometry is a powerful technique for determining which channel endohedral fullerenes follow in their unimolecular reactions. In MIKE spectra the peak position of a daughter ion U_d is closely related to that of its parent ion U_p by Equation (1),

$$U_d/U_p = (m_d Z_p)/(m_p Z_d) \quad (1)$$

where m_d and Z_d are the mass and charge of the daughter ion, and m_p and Z_p are the mass and charge of the parent ion. In our current studies both the parent and daughter ions are singly charged ($Z_d = Z_p = 1$).

Peak positions of the metastable and parent ions measured from the MIKE spectra for C_{70}^+ and $N@C_{70}^+$ are listed in Table 1. Knowing the masses of parent ions we se-

Table 1. Peak positions and corresponding masses of parent and metastable daughter ions. U_p and m_p (U_d and m_d) are the peak position and mass of parent ion (daughter ion), respectively.

Parent ions	m_p [amu]	U_p [eV]	U_d [eV]	m_d [amu]	$m_p - m_d$ [amu]
C_{70}^+	840	8208	7973	816	24
$N@C_{70}^+$	854	8203	8069	840	14
$N@C_{60}^+$	734	7197	7059	720	14

lected in the experiment, the corresponding masses of daughter ions were calculated by using Equation (1) (see Table 1). From Table 1 it is clear that $N@C_{70}^+$ emits the endohedral N atom in its unimolecular decomposition, which is in sharp contrast with C_{70}^+ that expels a C_2 unit. No other decomposition channels were detected for $N@C_{70}^+$. Exactly the same situation was found for C_{60}^+ and its endohedral cation $N@C_{60}^+$.[6] The unimolecular dissociation channels for C_{70}^+ and $N@C_{70}^+$ cations are shown in Equations (2) and (3).

$$C_{70}^+ \rightarrow C_{68}^+ + C_2 \quad (2)$$

$$N@C_{70}^+ \rightarrow C_{70}^+ + N \quad (3)$$

We first carried out a preliminary study[19] and then thorough studies of unimolecular decompositions of endohedral fullerene cations using tandem mass spectrometry.[6,19–21] Among the compounds studied were $Ne@C_{60}$, $Ar@C_{60}$, $Kr@C_{60}$, $N@C_{60}$, $N_2@C_{60}$, $N@C_{70}$, $Ne@C_{70}$, $Ar@C_{70}$, $N_2@C_{70}$, $La@C_{82}$, $T_b@C_{82}$, $Ti_2@C_{80}$, $Sc_2@C_{84}$, and $Sc_3N@C_{80}$. All these endohedral cations expel C_2 units and undergo cage shrinking in unimolecular reactions, except $N@C_{60}^+$ and $N@C_{70}^+$, which instead lose the endohedral atom. The phenomenon that unimolecularly decomposing endohedral fullerenes expel the encapsulated atom rather than a C_2 unit is thus unique to N-containing fullerenes.

Kinetic energy release: Unimolecular reactions that have no reverse activation energies lead to kinetic energy release distributions that are Boltzmann-like.[17–20] The MIKE spectra for unimolecular decomposition reveal kinetic energy release distributions (KERDs) in the reaction.[17–20] The experimental KERDs are determined from the first derivatives of the peak shapes of the metastable ions (MIKE spectra).[17] If the MIKE spectra are Gaussian, the KERDs deduced from both the left and right sides of the spectra will be Boltzmann-like and, in a model-free approach developed by Klots,[22] the KERD is written in the form of Equation (4),

$$p(\varepsilon) = \varepsilon^l \exp(-\varepsilon/k_B T^{\neq}) \quad (4)$$

where ε is the kinetic energy release, l is a parameter that ranges from zero to unity depending on the interaction potential between the fragments, k_B is Boltzmann's constant, and $T^{\neq}$ is the transition-state temperature defined by the average kinetic energy on passing through the transition state. The values of l and $T^{\neq}$ can be deduced by fitting the experimental KERD with Equation (4) by nonlinear regression.

The value of l which gave the best fit to all the KERDs generated from the Gaussian MIKE spectra was $l = 0.5$. This corresponds to the expected value for the most statistical situation, since the translational density of states is proportional to $\varepsilon^{0.5}$.[22] This is the case for the present study. Since our metastable- and parent-ion peak shapes are all Gaussian (see Figures 2 and 3), the KERDs generated from the MIKE spectra are readily modeled by a parameter-free approach using Equation (4). The typical center-of-mass product KERDs for reactions (2) and (3) together with their nonlinear regression fits are shown in Figure 4. The solid

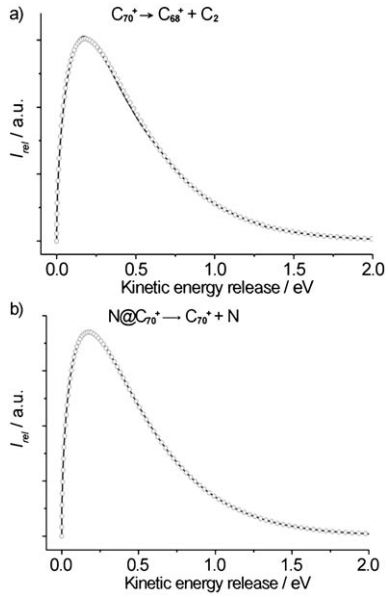

Figure 4. Kinetic energy release distributions (KERDs) deduced from the metastable-peak shapes for reactions a) $C_{70}^+ \rightarrow C_{68}^+ + C_2$ and b) $N@C_{70}^+ \rightarrow C_{70}^+ + N$. Solid line: experimental, open circle: fit based on Equation (4).

lines represent the experimental curves, and the open circles the fits. The modeled KERDs are superimposed on the experimental ones. The l parameter obtained from the fit is 0.50 ± 0.01 for both C_{70}^+ and $N@C_{70}^+$. The transition-state temperatures $T^{\neq}$ deduced from KERDs for reactions (2) and (3) are 3326 and 3644 K, respectively. Details of the fit parameters are listed in Table 2.

Table 2. Transition-state temperatures $T^{\neq}$, average kinetic energy releases ε_{av}, C_2 binding energies ΔE_{vap}, and activation energies for N loss deduced from KERDs by using finite heat bath theory.

Parent ion	$T^{\neq}$ [K]	T_B [K]	l	ε_{av} [eV]	ΔE_{vap} [eV]
C_{70}^+	3326	3610[a]	0.50	0.43	10.3 ± 0.4[a]
$N@C_{70}^+$	3644	3866,[b] 3730[c]	0.50	0.47	8.0,[b] 3.0 ± 0.4[c]
$N@C_{60}^+$	3954	4239,[d] 4065[e]	0.50	0.51	8.9,[d] 3.4 ± 0.3[e]

[a] $\gamma = 33$. [b] $\gamma = 24$. [c] $\gamma = 9.48$. [d] $\gamma = 24.3$. [e] $\gamma = 9.7$.

Activation energies for N extrusion from $N@C_{70}^+$ and for C_2 evaporation from C_{70}^+: The isokinetic bath temperature T_b is defined in finite heat bath theory as the temperature to which a heat bath should be set so that the canonical rate constant $k(T_b)$ is equal to the microcanonical rate constant $k(E)$ sampled in the experiment.[23] It is calculated by Equation (5),[23–25]

$$T_b = T^{\ddagger} C[\exp(\gamma/C)-1]/\gamma \quad (5)$$

where $T^{\ddagger}$ is the transition-state temperature deduced by fitting the experimental KERDs; C the heat capacity of the parent ion, given by $C=3n-6$, where n is the total number of atoms in the parent ion; and γ the Gspann parameter.[23,25] The currently accepted value of the Gspann parameter for C_2 loss from fullerene cations is $\gamma=33$.[19–20,25] This γ value has been adopted for the unimolecular decomposition of endohedral fullerene cations as well.[19–20] Here we also employ this γ value for data analysis on the KERDs in the unimolecular C_2-loss reaction of C_{70}^+.

In finite heat bath theory the activation energy ΔE_{vap} for unimolecular reaction is well established. It is calculated from the isokinetic bath temperature T_b via the Trouton relation [Eq. (6)].[19,25]

$$\Delta E_{vap} = \gamma k_B T_b \quad (6)$$

The average kinetic energy release is related to the transition temperature $T^{\ddagger}$ by Equation (7),[25]

$$\varepsilon_{av} = (1+l)k_B T^{\ddagger} \quad (7)$$

where ε_{av} is the average kinetic energy release. All the parameters obtained by parameter-free modeling of the KERDs are listed in Table 2.

Using finite heat bath theory and Gspann parameter $\gamma=33$, the binding energy for C_2 loss from C_{70}^+ extracted from the KERDs of reaction (2) is 10.3 ± 0.4 eV. Under the same conditions the C_2 evaporation energy of C_{60}^+ is measured to be 11.1 ± 0.4 eV, which is much larger than that from C_{70}^+, that is, it could be much easier to break a bond to open a window in C_{70} than in C_{60}. This is consistent with our finding that the N atom is more readily encapsulated into C_{70} than into C_{60}.

Deducing the activation energy for N elimination from $N@C_{70}^+$ is more sophisticated, because the γ value for loss of an endohedral atom has not been well-established yet. We extracted information on the evaporation energy for N elimination from $N@C_{70}^+$ as follows. First we conclude that the activation energy for N loss should be less than the C_2 binding energy. In principle, there would be competition in the unimolecular reaction of $N@C_{70}^+$ between elimination of the endohedral N atom [channel (3)] and loss of the C_2 unit [channel (8)].

$$N@\quad C_{70}^+ \rightarrow N@\quad C_{68}^+ + C_2 \quad (8)$$

Through which channel $N@C_{70}^+$ decomposes depends on the activation energies of the two channels. Here we found on the basis of MIKE spectroscopic analysis that $N@C_{70}^+$ expels the N atom, not the C_2 unit, that is, the activation energy for N escape is unambiguously lower than that for C_2 loss ($\Delta E_{vap}(N@C_{70}^+, N) < \Delta E_{vap}(N@C_{70}^+, C_2)$).

Second, we compared $\Delta E_{vap}(C_{70}^+, C_2)$ with $\Delta E_{vap}(N@C_{70}^+, C_2)$. It is impossible to measure the binding energy for C_2 elimination from $N@C_{70}^+$, because this channel never happens in our experiment. However, $\Delta E_{vap}(C_{70}^+, C_2)$ is available. Here we assume that there should be no big difference in C_2 binding energy between C_{70}^+ and $N@C_{70}^+$ for the following two reasons: 1) We recently determined the C_2 evaporation energies for C_{70}^+, $Ne@C_{70}^+$, and $Ar@C_{70}^+$ and found they are almost identical within experimental uncertainty.[21a] There are many similarities among $N@C_{70}$, $Ne@C_{70}$, and $Ar@C_{70}$: all the endohedral atoms occupy the center position of C_{70}; no electron transfer occurs within these molecules; no covalent bonding between the endohedral atom and its accommodation exists; and all the endohedral atoms are in their atomic state. It is therefore very likely that the C_2 emission energies for C_{70}^+ and $N@C_{70}^+$ are nearly equal, like C_{70}^+, $Ne@C_{70}^+$, and $Ar@C_{70}^+$. 2) We measured the MIKE spectra of $N_2@C_{70}^+$ and determined its dissociation channel. $N_2@C_{70}^+$ follows the Rice shrink-wrap mechanism like normal fullerenes. Our preliminary analysis of the KERDs of $N_2@C_{70}^+$ resulted in nearly the same C_2 binding energy as C_{70}^+ as well.[21b] It would be difficult to imagine that the contribution of a nitrogen atom to the C_2 binding of C_{70} is more than that of an N_2 molecule in the absence of either a chemical bond or electron transfer happened between guest and cage. Based on the above analysis the evaporation energy for N extrusion from $N@C_{70}^+$ should be less than the C_2 binding energy in C_{70}^+ as well, that is, $\Delta E_{vap}(N@C_{70}^+, N) < \Delta E_{vap}(N@C_{70}^+, C_2) \approx \Delta E_{vap}(C_{70}^+, C_2) = 10.3$ eV.

Finally, in terms of looseness of the transition state and using the well-established parameters for C_2 loss from C_{70}^+, we can deduce the upper and lower limits of the activation energy for N elimination in reaction (3). In finite heat bath theory the Gspann parameter γ defines the degree of looseness of the transition state as Equation (9),[22–23,25]

$$\gamma = \ln A - \ln k(T_b) \quad (9)$$

where A is the Arrhenius preexponential factor, and $k(T_b)$ the canonical rate constant at temperature T_b. Fullerenes and metallofullerenes have been demonstrated to have a very loose transition state with a high γ value of $\gamma=33$ for C_2 loss.[18–21] This γ value was adopted for C_2 loss from C_{70}^+ in reaction (2). Since the Arrhenius preexponential factor includes the reaction path degeneracy σ and the partition function δ for the C_2 fragment,[25a] the γ value for N extrusion in reaction (3) should definitely be lower than the γ value for C_2 loss in reaction (2). The reason for this is that in reaction (2) of C_{70}^+ there are 70 ways of choosing the reaction coordinate ($\sigma=70$) and 105 ways for partitioning the

C_2 unit ($\delta = 105$), but there is only one N atom to be lost in reaction (3). This argument is based on the assumption that all the carbon atoms in C_{70} are equal. One might argue that the carbon atoms in C_{70} are not all the same and the C–C bonds are not all equivalent, because most organic additions to C_{70} found so far occur at the ends, where curvature and strain are greatest.[26a] This is the case at lower temperature, say, a couple of hundred degrees Celsius (most organic additions were carried out below 250 °C),[26a] but at high temperatures (above 3000 K) like those at which fullerene dissociation reactions take place (cf. $T^{\ddagger}$ and T_B in Table 1), the non-equivalence of the C–C bonds is broken. A tight-binding molecular dynamics approach toward the fragmentation of fullerenes demonstrates that at about 3000 K the C_{60} and C_{70} molecules form a floppy phase with fluctuations in C–C bond lengths as large as ± 0.4 Å but do not disintegrate.[26b] With respect to the C–C bond lengths of C_{70} at room temperature (1.37–1.46 Å),[26c] these fluctuations could modify the bond length by nearly $\pm 29\,\%$. In the floppy phase the curvature and strain at the ends of C_{70} are significantly reduced, and those around the center belt are considerably increased, which makes all the C–C bonds and atoms almost identical. The higher the temperature of the fullerene molecules is, the more the C–C bonds fluctuate. This computational approach demonstrated that the cage structure of fullerene is maintained in the floppy phase till about 4000 K, at which fragmentation occurs and, because of the equivalence of C–C bonds achieved, not only C_2 loss but possibly C_4 and C_5 loss as well could be observed.[26c] Therefore, it is rational to treat the carbon atoms equally in our high-temperature system. Taking the reaction-path degeneracy σ and partition function δ into account, the γ value for reaction (3) should be equal to $\gamma(2) - \ln 70 - \ln 105 = 24$. With this γ value one can obtain the activation energy for reaction (3) from Equations (5) and (6): $\Delta E_{vap}(N@C_{70}^+, N) = 8.0$ eV. This value serves as an upper limit for the activation energy in reaction (3).

The γ value of 24 discussed above for N loss from $N@C_{70}^+$ corresponds to an Arrhenius preexponential factor of $A = 2.6 \times 10^{15}\ s^{-1}$, as the most probable rate constant $k(T_b)$ is about $10^5\ s^{-1}$, characteristic of the instrument.[24] Such a high A factor is deduced by assuming that $N@C_{70}^+$ has a transition state as loose as that of C_{70}^+. This seems very unlikely for reaction (3), because the much narrower MIKE spectra of $N@C_{70}^+$ compared to C_{70}^+ (see Figure 5) suggest that the transition state for the dissociation of $N@C_{70}^+$ has a low degree of looseness. The fact that the transition state in the unimolecular reaction $N@C_{70}^+ \rightarrow C_{70}^+ + N$ is not as loose as that in the reaction $C_{70}^+ \rightarrow C_{68}^+ + C_2$ is confirmed by a theoretical approach to the thermal stability of $N@C_{70}$.[27] The lowest pre-exponential factor that has been determined for C_{70}^+ is $A = 10^{13}\ s^{-1}$, which represents a lower degree of looseness.[25a] With this factor we obtained a smaller Gspann parameter for N extrusion in reaction (3) of $\gamma(3) = 9.48$. Using this γ value one obtains a lower limit of the activation energy for reaction (3) of $\Delta E_{vap}(N@C_{70}^+, N) = 3.0$ eV. Our KERD measurements place the activation energy for N extrusion from $N@C_{70}^+$ in the range $3.0\ \text{eV} \le \Delta E_{vap}(N@C_{70}^+, N) \le 8.0$ eV. This value is considerably lower than the C_2 binding energy of $N@C_{70}^+$ ($\Delta E_{vap}(N@C_{70}^+, C_2) \approx 10.3$ eV), as expected, and provides an explanation why $N@C_{70}^+$ expels the N atom rather than a C_2 unit.

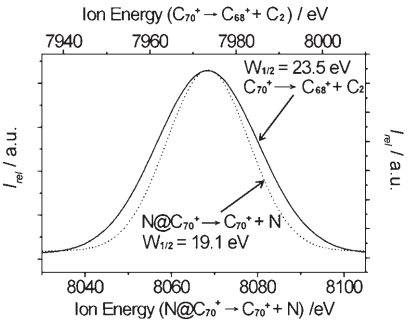

Figure 5. Widths of MIKE spectra at half height for reactions $C_{70}^+ \rightarrow C_{68}^+ + C_2$ (top x and right y axes) and $N@C_{70}^+ \rightarrow C_{70}^+ + N$ (bottom x and left y axes). The two spectra are normalized and drawn to the same laboratory energy scale. With respect to the daughter ion of C_{70}^+, the width of the metastable peak of $N@C_{70}^+$ is much smaller.

We applied the same method to reevaluate the previously measured activation energy for $N@C_{60}^+$,[6] which is too high with respect to the theoretical value.[27–28] Similar to the case of $N@C_{70}^+$, the metastable ion peak in the unimolecular dissociation of $N@C_{60}^+$ is much narrower than that of C_{60}^+ (see Figure 6), and this provides proof that the fragmentation of $N@C_{60}^+$ has a transition state with a low degree of looseness as well. We reprocessed the previous measured data of $N@C_{60}^+$[6] (see Table 2) in the same way discussed above. Re-analysis of the KERDs positions the activation energy for N exclusion from $N@C_{60}^+$ in the range $3.5\ \text{eV} < \Delta E_{vap}(N@C_{60}^+, N) < 8.9$ eV, which is significantly lower than the C_2 binding energy of $N@C_{60}^+$ ($\Delta E_{vap}(N@C_{60}^+, C_2) \approx \Delta E_{vap}(C_{60}^+, C_2) = 11.1$ eV) and reveals the reason why $N@C_{60}^+$ dissociates by loss of the N atom rather than a C_2 unit, though the evaporation energies of C_2 from $N@C_{60}^+$ and C_{60}^+ may not be necessarily equal. This newly reevaluated

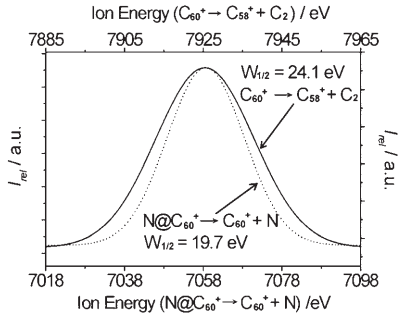

Figure 6. Widths of MIKE spectra at half height for reactions $C_{60}^+ \rightarrow C_{58}^+ + C_2$ (top x and right y axes) and $N@C_{60}^+ \rightarrow C_{60}^+ + N$ (bottom x and left y axes). The two spectra are normalized and drawn to the same laboratory energy scale. With respect to the daughter ion of C_{60}^+, the width of the metastable peak of $N@C_{60}^+$ is much smaller.

value is much lower than the previous one and coincides with the theoretically calculated value.[28–29]

Our observation that $N@C_{70}^+$ extrudes unimolecularly the endohedral N atom rather than a C_2 unit is completely consistent with the thermal stability of its neutral molecule.[29] Whereas relatively mild heating of the N-containing endohedral fullerenes leads to release of the nitrogen atom from the cage, extrusion of He from its endohedral fullerenes requires thermal treatment above 1100 K for hours and is accompanied by irreversible destruction of the fullerene cage.[30] It has been computationally demonstrated that extrusion of He from its endohedral fullerenes by the window mechanism without chemical bonding with the cage requires overcoming an energy barrier of at least 11.8 eV,[31] which is much higher than the measured C_2 binding energy of the cage. This is the reason why noble-gas-containing C_{60} and C_{70} expel a C_2 unit rather than the endohedral atom in their unimolecular reactions. If the N atom left the cage without any bonding with the cage, we would have detected not N elimination but the C_2 loss, like in $Ne@C_{70}^+$ and $Ar@C_{70}^+$, and the activation energy for N extrusion would have not been so low. Our MIKE spectra and measured low activation energies of the reactions strongly suggest that the N atom does not escape from the fullerene cages by the no-bonding window mechanism. Hirsch et al. demonstrated computationally that the N atom flees the cage via formation of an intermediate with an endohedral aza bridge between the N atom and the cage, which greatly lowers the energy barrier.[27] Our results support this aza-bridge mechanism. Based on this mechanism, theoretical calculations at the MP3-UHF level on the potential for elimination of the N atom from neutral $N@C_{60}$ place the activation energy in the range $2.7\,eV \leq \Delta E_{vap}(N@C_{60}^+, N) \leq 3.8\,eV$.[27–28] Experimental investigations on annealing behaviors of neutral $N@C_{60}$ and $N@C_{70}$ by Weidinger et al. give much lower activation energies: 1.57 eV for $N@C_{60}$ and 1.39 eV for $N@C_{70}$.[28] The activation energies deduced from our KERD measurements are higher than these values, but coincide with the theoretical ones.[27–28] The discrepancies mentioned above may originate from the different electronic states of the starting materials. Our data were measured for the reactions of $N@C_{70}^+$ and $N@C_{60}^+$ cations, whereas the theoretical and thermal-reaction values were calculated for the dissociation of neutral $N@C_{60}$ and $N@C_{70}$ molecules. Because of the highly electronegative and electrophilic nature of the N atom, one can imagine that it should be much easier for N to construct an aza bond with the neutral C_{70} and C_{60} cages rather than with the C_{70}^+ and C_{60}^+ cations. Therefore, it is rational that the energy barrier for the N atom to flee from the neutral cage is much lower than that from the positively charged accommodation. The N-containing endohedral fullerene cations are more thermally stable than their neutral molecules. In other words, the discrepancy discussed above further verifies that the N-extrusion mechanism via an aza-bridged intermediate[27–28] is correct.

We found here that the activation energy for N extrusion from $N@C_{70}^+$ is lower than that from $N@C_{60}^+$. This indicates that $N@C_{70}^+$ is less stable than $N@C_{60}^+$, which is consistent with the conclusions on the basis of thermal stability analyses on $N@C_{60}$ and $N@C_{70}$.[28] $N@C_{70}$ starts to decay on heating at around 450 K, whereas $N@C_{60}$ retains its endohedral structure until 500 K. A physicochemical reason for this stems probably from the discrepancy in C_2 binding energy between C_{60}^+ and C_{70}^+. The fact that the C_2 binding energy for C_{70}^+ is lower than that for C_{60}^+ suggests it could be easier to partially break the bond for formation of the aza intermediate in C_{70}^+ than in C_{60}^+, and therefore the N atom should more readily escape from the C_{70}^+ cage than from the C_{60}^+ cage.

Conclusion

The unimolecular decompositions of C_{70}^+ and $N@C_{70}^+$ have been studied by tandem mass spectrometry techniques. Information on the energetics and dynamics of the reaction has been extracted. The C_{70}^+ ion undergoes a cage-shrinking reaction by C_2 loss whereas $N@C_{70}^+$ emits the endohedral atom. The cage C_2 binding energies determined from the kinetic energy release distributions in unimolecular decomposition of C_{70}^+ are much higher than the activation energy for N escape from $N@C_{70}^+$. Reevaluation of the previously measured data for the unimolecular reaction of $N@C_{60}^+$ gave similar results to $N@C_{70}^+$. The measured activation energies for extrusion of the N atom from $N@C_{60}^+$ and $N@C_{70}^+$ cations are higher than the values for neutral $N@C_{60}$ and $N@C_{70}$ molecules, which is consistent with the N-escape mechanism via an aza-bridged intermediate.

Experimental Section

The production and isolation of C_{70} have been published elsewhere.[31] In brief, soot containing fullerenes was generated by the dc arc-discharge method. A graphite rod (chromatographic grade, $\varnothing$ 4.6×130 mm, Tokyo Tenso Co.) was vaporized by dc arc under 150 torr flowing He atmosphere. The optimized arc-discharge conditions for high-yield production of C_{70} are as follows: dc current 150 A, discharge voltage 35 V, baking current 100 A, baking time 20 min. The soot was collected under protection of Ar. The mixture of fullerenes was extracted from the soot with 1,2,4-trichlorobenzene at reflux under Ar overnight. After removal of the solvent, the fullerene mixture was dissolved in toluene for HPLC separation. A PYE column was employed for isolation of C_{70} ($\varnothing$ 20×250 mm, eluant: toluene, room temperature, flow rate 10 mL min^{-1}). The C_{70} sample thus obtained was confirmed to be free of C_{60} and higher fullerenes by HPLC and mass spectroscopic analyses.

$N@C_{70}$ was prepared by bombarding C_{70} with N^+ ion beams generated by an electrical discharge. Details of the generation apparatus have been published previously.[32] Briefly, the doping process takes place in a vacuum chamber equipped with a rotating aluminum cylinder at the center, a resistance oven on one side, and an arc-discharge filament on the other. The oven produces a continuous beam of C_{70} by sublimation, which condenses on the cold cylinder. The nitrogen-ion beam is generated by passing N_2 through the electrical discharge. Before collision with the target, the N^+ ions are extracted from neutral species by an ion lens, bent by 30°, accelerated to 200 eV, then slam into the C_{70} surface freshly deposited on the aluminum cylinder. After a few hours, the apparatus is opened, and the target is removed and washed with CS_2. About 100 mg

of pure C_{70} was vaporized onto the cylinder, and about 70 mg of extract was retrieved with a doping yield of ca. 0.3 %.

Measurements of parent- and metastable-ion peaks were carried out on a high-resolution double-focusing VG-ZAB-2F mass spectrometer of reversed geometry recording mass spectra with a very high dynamic range and using the technique of mass-analyzed ion kinetic energy (MIKE) spectrometry.[24] Details of the instruments and measurement conditions have been described previously.[19] Briefly, the endohedral fullerene cations were obtained by ionization of the corresponding neutral samples, which were introduced into the mass spectrometer by using a direct insertion probe. The electron-impact conditions for ionizing the samples were as follows: electron ionizing energy 70 eV, emission current 5 mA, ion-source temperature 200 °C, resolution 1100 (10 % valley definition). Peak shapes of metastable ions were determined by scanning an electrostatic analyzer and single-ion counting with a combination of an electron multiplier, amplifier/discriminator, and multichannel analyzer.[18] The experiments were performed at an acceleration voltage of 8 kV and a main-beam width of 3–5 V. The data were accumulated in a computer-controlled experiment with monitoring of the main-beam scan and correcting for the drift of the main beam.[24] Peak shapes of metastable ions were the mean values of 100–1000 accumulated scans. The product kinetic energy release distributions (KERDs) were determined from the first derivatives of peak shapes of metastable ions.[17]

Acknowledgement

R.J.C. and M.S. thank the National Science Foundation for financial support. B.C. thanks the Hebrew University for the award of a Golda Meir Fellowship. This research is partially supported by the Hebrew University Intramural Research Fund Basic Project Awards. We thank the Austrian Friends of the Hebrew University. The Farkas Research Center is supported by the Minerva Gesellschaft für die Forschung GmbH München.

[1] a) T. Weiske, D. K. Böhme, J. Hrusäk, W. Krätschmer, H. Schwarz, *Angew. Chem.* **1991**, *103*, 898; *Angew. Chem. Int. Ed. Engl.* **1991**, *30*, 884; b) T. Weiske, J. Hrusäk, D. K. Böhme, H. Schwarz, *Helv. Chim. Acta* **1992**, *75*, 79; c) T. Weiske, T. Wong, W. Krätschmer, J. K. Terlouw, H. Schwarz, *Angew. Chem.* **1992**, *104*, 242; *Angew. Chem. Int. Ed. Engl.* **1992**, *31*, 183.

[2] a) M. Saunders, H. A. Jiménez-Vázquez, R. J. Cross, R. J. Poreda, *Science* **1993**, *259*, 1428; b) M. Saunders, H. A. Jiménez-Vázquez, R. J. Cross, S. Mroczkowski, D. I. Freedberg, F. A. L. Anet, *Nature* **1994**, *367*, 256; c) M. Saunders, R. J. Cross, H. A. Jiménez-Vázquez, R. Shimshi, A. Khong, *Science* **1996**, *271*, 1693.

[3] a) R. Teligmann, N. Krawez, S. Lin, I. V. Hertel, E. E. P. Campbell, *Nature* **1996**, *382*, 407; b) R. Shimshi, R. J. Cross, M. Saunders, *J. Am. Chem. Soc.* **1997**, *119*, 1163; c) R. J. Cross, M. Saunders, H. Prinzbach, *Org. Lett.* **1999**, *1*, 1479.

[4] L. Becker, R. J. Poreda, J. L. Bada, *Science* **1996**, *272*, 249.

[5] a) Y. Rubin, T. Jarrosson, G. Wang, M. D. Bartberger, G. Schick, M. Saunders, R. J. Cross, K. N. Houk, *Angew. Chem.* **2001**, *113*, 1591; *Angew. Chem. Int. Ed.* **2001**, *40*, 1543; b) Y. Murata, M. Murata, K. Komatsu, *J. Am. Chem. Soc.* **2003**, *125*, 7152; c) K. Komatsu, M. Murata, Y. Murata, *Science* **2005**, *307*, 238.

[6] B. Cao, T. Peres, A. Khong, Jr., R. J. Cross, M. Saunders, C. Lifshitz, *J. Phys. Chem. A* **2001**, *105*, 2142.

[7] a) T. Almeida Murphy, T. Pawlik, H. Höhne, R. Alcala, J. M. Spaeth, *Phys. Rev. Lett.* **1996**, *77*, 1075; b) B. Pietzak, M. Waiblinger, T. Almeida Murphy, A. Weidinger, M. Höhne, E. Dietel, A. Hirsch, *Chem. Phys. Lett.* **1997**, *279*, 259; c) C. Knapp, K.-P. Dinse, B. Pietzak, M. Waiblinger, A. Weidinger, *Chem. Phys. Lett.* **1997**, *272*, 433; d) B. Pietzak, M. Waiblinger, T. Almeida Murphy, A. Weidinger, M. Höhne, E. Dietel, A. Hirsch, *Carbon* **1998**, *36*, 613; e) N. Weiden, H. Käss, K.-P. Dinse, *J. Phys. Chem. B* **1999**, *103*, 9826.

[8] a) C. Knapp, N. Weiden, H. Käb, K.-P. Dinse, B. Pietzak, M. Waiblinger, A. Weidinger, *Mol. Phys.* **1998**, *95*, 999; b) A. Weidinger, M. Waiblinger, B. Pietzak, T. Almeida Murphy, *Appl. Phys. A* **1998**, *66*, 287; c) E. Dietel, A. Hirsch, B. Pietzak, M. Waiblinger, A. Gruss, K.-P. Dinse, *J. Am. Chem. Soc.* **1999**, *121*, 2432; d) P. Jakes, N. Weiden, R.-A. Echel, A. Gembus, K.-P. Dinse, C. Meyer, W. Harneit, A. Weidinger, *J. Magn. Reson.* **2002**, *156*, 303.

[9] a) K. Lips, M. Waiblinger, B. Pietzak, A. Weidinger, *Phys. Stat. Sol.* **2000**, *177*, 81; b) S. Biri, A. Valek, L. Kenéz, A. Jánossy, A. Kitagawa, *Rev. Sci. Instrum.* **2002**, *73*, 881; c) C. Meyer, W. Hareit, K. Lips, A. Weidinger, P. Jakes, K.-P. Dinse, *Phys. Rev. A* **2002**, *65*, 061201; d) F. Simon, H. Kuzmany, H. Rauf, T. Pichler, J. Bernardi, H. PeterliK, L. Korecz, F. Fölöp, A. Jänossy, *Chem. Phys. Lett.* **2004**, *383*, 362; e) M. Ata, H. Huang, T. Akasaka, *J. Phys. Chem. B* **2004**, *108*, 4640.

[10] a) J. C. Greer, *Chem. Phys. Lett.* **2000**, *326*, 567; b) J. A. Larsson, J. C. Greer, W. Harneit, A. Weidinger, *J. Chem. Phys.* **2002**, *116*, 7849; c) K. Kobayashi, S. Nagase, K.-P. Dinse, *Chem. Phys. Lett.* **2003**, *377*, 93; d) B. N. Plakhutin, N. N. Blaslavskaya, E. V. Gorelik, A. V. Arbuznikov, *J. Mol. Struc. THEOCHEM.* **2005**, *727*, 149.

[11] a) N. Weiden, B. Goedde, H. Käβ, K.-P. Dinse, *Phys. Rev. Lett.* **2000**, *85*, 00319007; b) K.-P. Dinse, *Phys. Chem. Chem. Phys.* **2002**, *4*, 5442.

[12] a) D. Suter, K. Lim, *Phys. Rev. A* **2002**, *65*, 052309; b) W. Harneit, *Phys. Rev. A* 2002, 65, 32322.

[13] a) T. Suetsuna, N. Dragoe, W. Harneit, A. Weidinger, H. Shimotani, S. Ito, H. Takagi, K. Kitazawa, *Chem. Eur. J.* **2002**, *8*, 5079; b) P. Jakes, K.-P. Dinse, C. Meyer, W. Harneit, A. Weidinger, *Phys. Chem. Chem. Phys.* **2003**, *5*, 4080.

[14] M. Kanai, K. Porfyrakis, G. A. D. Briggs, T. J. S. Dennis, *Chem. Commun.* **2004**, 210.

[15] T. Wakahara, Y. Matsunaga, A. Katayama, Y. Maeda, M. Kato, T. Akasaka, M. Okumura, T. Kato, Y.-K. Choe, K. Kobayashi, S. Nagase, H. Huang, M. Ata, *Chem. Commun.* **2003**, 2940.

[16] T. Peres, B. Cao, W. Cui, A. Khong, R. J. Cross, M. Saunders, C. Lifshitz, *Int. J. Mass Spectrom.* **2001**, *210/211*, 241.

[17] a) J. L. Holmes, A. D. Osborne, *Int. J. Mass Spectrom. Ion Phys.* **1977**, *23*, 189; b) C. Lifshitz, E. Tzidony, *Int. J. Mass Spectrom. Ion Phys.* **1981**, *39*, 181; c) M. F. Jarrold, W. Wagner-Redeker, A. J. Allies, N. J. Kirchner, M. T. Bowers, *Int. J. Mass Spectrom. Ion Processes* **1984**, *58*, 63.

[18] C. Lifshitz, F. Louage, *J. Phys. Chem.* **1989**, *93*, 6533.

[19] a) J. Laskin, B. Hadas, T. D. Märk, C. Lifshitz, *Int. J. Mass Spectrom.* **1998**, *177*, L9; b) J. Laskin, T. Peres, A. Khong, H. A. Jiménez-Vázquez, M. Saunders, R. J. Cross, C. Lifshitz, *Chem. Phys. Lett.* **1995**, *242*, 249; c) J. Laskin, H. A. Jiménez-Vázquez, R. Shimishi, M. Saunders, M. S. der Vries, C. Lifshitz, *Int. J. Mass Spectrom.* **1999**, *185/186/187*, 61; d) S. Tomita, J. U. Anderson, C. Gottrup, U. V. Pederson, *Phys. Rev. Lett.* **2001**, *87*, 073401.

[20] a) J. Laskin, T. Peres, C. Lifshitz, M. Saunders, R. J. Cross, A. Khong, *Chem. Phys. Lett.* **1998**, *285*, 7; b) T. Peres, B. Cao, H. Shinohara, C. Lifshitz, *Int. J. Mass Spectrom.* **2003**, *228*, 181; c) K. Gluch, S. Feil, S. Matt-Leubner, O. Echt, P. Scheier, T. D. Märk, *J. Phys. Chem. A* **2004**, *108*, 6990.

[21] a) B. Cao, T. Peres, R. J. Cross, M. Saunders, C. Lifshitz, *J. Phys. Chem. A*, in press; b) B. Cao, T. Peres, R. J. Cross, M. Saunders, C. Lifshitz, $\Delta E_{vap}(N_2@C_{70}^+, C_2) = 10.1 \pm 0.9$ eV.

[22] a) C. E. Klotz, Z, *Phys. D* **1991**, *21*, 335; b) T. Baer, W. L. Hase, *Unimolecular Reaction Dynamics*, Oxford University, New York, **1996**, pp. 173–174; c) P. Urbain, F. Remacle, B. Leyh, J. C. Lorquet, *J. Phys. Chem.* **1996**, *100*, 8003.

[23] a) C. E. Klotz, *J. Chem. Phys.* **1989**, *90*, 4470; b) C. E. Klotz, *Int. J. Mass Spectrom. Ion Processes* **1990**, *100*, 457.

[24] a) P. P. Morgan, J. H. Beynon, R. H. Bateman, B. N. Green, *Int. J. Mass Spectrom. Ion Phys.* **1978**, *28*, 171; b) N. J. Kirshner, M. T. Bowers, *J. Phys. Chem.*, **1987**, *91*, 2573.

[25] a) C. Lifshitz, *Int. J. Mass Spectrom.* **2000**, *198*, 1; b) J. Laskin, C. Lifshitz, *Int. J. Mass Spectrom.* **2001**, *36*, 459; c) S. Matt, O. Echt, M. Sonderegger, R. David, P. Scheier, J. Laskin, C. Lifshitz, T. D. Märk, *Chem. Phys. Lett.* **1999**, *303*, 379; d) K. Gluch, S. Matt-Leubner, L.

Michalark, O. Echt, A. Stamatovic, P. Scheier, T. D. Märk, *J. Chem. Phys.* **2004**, *120*, 2686.

[26] a) K. M. Kadish, R. S. Ruoff, *Fullerenes: Chemistry, Physics and Technology*, Wiley, New York, **2000**; b) E. Kim, D.-H. Oh, C. W. Oh, Y. H. Lee, *Synth. Met.* **1995**, *70*, 1495; c) M. Fujita, N. Kurita, K. Nakao, *Synth. Met.* **1995**, *70*, 1509.

[27] H. Mauser, N. J. R. van Eikema Hommes, T. Clark, A. Hirsch, B. Pietzak, A. Weidinger, L. Dunsch, *Angew. Chem.* **1997**, *109*, 2858; *Angew. Chem. Int. Ed. Engl.* **1997**, *36*, 2835.

[28] M. Weiblinger, K. Lips, W. Harneit, A. Weidinger, E. Dietel, A. Hirsch, *Phys. Rev. B* **2001**, *63*, 045421, **2001**, 64, 159901 (E).

[29] R. Shimshi, A. Khong, H. A. Jiménez-Vázquez, R. J. Cross, M. Saunders, *Tetrahedron* **1996**, *52*, 5143.

[30] a) M. Kolb, W. Thiel, *J. Comput. Chem.* **1993**, *14*, 37; b) S. Patchkovskii, W. Thiel, *J. Am. Chem. Soc.* **1996**, *118*, 7164.

[31] a) B. Cao, T. Wakahara, T. Tsuchiya, M. Kondo, Y. Maeda, G. M. A. Rahman, T. Akasaka, K. Kobayashi, S. Nagase, K. Yamamoto, *J. Am. Chem. Soc.* **2004**, *126*, 9164; b) B. Cao, M. Hasegawa, K. Okada, T. Tomiyama, T. Okazaki, K. Suenaga, H. Shinohara, *J. Am. Chem. Soc.* **2001**, *123*, 9679.

[32] a) M. Saunders, H. A. Jiménez-Vázquez, R. J. Cross, S. Mroczkowski, M. L. Gross, D. E. Giblin, R. J. Poreda, *J. Am. Chem. Soc.* **1994**, *116*, 2193; b) A. Khong, H. A. Jiménez-Vázquez, M. Saunders, R. J. Cross, J. Laskin, T. Peres, C. Lifshitz, R. Strongen, A. B. Smith, *J. Am. Chem. Soc.* **1998**, *120*, 6380.

Received: September 9, 2005
Published online: January 13, 2006

